Water Reuse

© 2023 The Authors

Water Reuse Vol 13 No 2, 233 doi: 10.2166/wrd.2023.006

Internet of things with nanomaterials-based predictive model for wastewater treatment using stacked sparse denoising auto-encoder

S. Neelakandan[a], N. V. RajaSekhar Reddy[b], Ayman A. Ghfar[c], Sadanand Pandey[d], Siripuri Kiran[e] and P. Thillai Arasu[f,*]

[a] Department of Computer Science and Engineering, R.M.K. Engineering College, Chennai, India
[b] Department of Information Technology, MLR Institute of Technology, Hyderabad, Telangana, India
[c] Department of Chemistry, College of Science, King Saud University, P.O. Box 2455, Riyadh 11451, Saudi Arabia
[d] Department of Chemistry, College of Natural Science, Yeungnam University, 280 Daehak-Ro, Gyeongsan, Gyeongbuk 38541, Republic of Korea
[e] Department of CSE(Networks), Kakatiya Institute of Technology & Science, Warangal-15, Telangana, India
[f] College of Natural and Computational Science, Wollega University, Post Box No 395, Nekemte, Ethiopia
*Corresponding author. E-mail: thililaiarasu@wollegauniversity.edu.et

ABSTRACT

Wastewater is a serious concern for the environment. There is a substantial amount of toxins that are discharged continuously from several pharmacological companies that lead to serious damage to public health and the ecosystem. Present wastewater treatment technologies include primary, tertiary, and secondary treatments that remove numerous contaminants; but pollutants in the nanoscale range were hard to remove with these steps. Some of these include inorganic and organic pollutants, pathogens, pharmaceuticals, and pollutants of developing concern. The utility of nanoparticles was a promising solution to this issue. Nanoparticles have exclusive properties permitting them to potentially eliminate residual pollutants but being eco-friendly and inexpensive. This study develops a new Archimedes optimization algorithm (AOA) with Stacked Sparse Denoising Auto-Encoder (SSDAE) model, named AOA-SSDAE for wastewater management in the IoT environment. The presented AOA-SSDAE technique aims to predict wastewater treatment depending on the influent indicators. In the presented AOA-SSDAE technique, the IoT devices are initially employed for the data collection process and then data normalization is performed to transform the collected data into a uniform format. For the predictive process, the SSDAE model is employed in this paper. To improve the SSDAE model's prediction capability, the AOA-based hyperparameter tuning process is involved.

Key words: deep learning, internet of things, nanomaterials, parameter tuning, predictive model, wastewater treatment

HIGHLIGHTS

- AOA-SSDAE is a novel Archimedes optimization algorithm (AOA) model with Stacked Sparse Denoising Auto-Encoder (SSDAE) for wastewater management in the context of the Internet of Things (IoT).
- The AOA-SSDAE method presented here aims to forecast wastewater treatment based on indicators of the influent.
- In the provided AOA-SSDAE methodology, IoT devices are initially used for data collection, followed by data normalization to convert the collected data into a standard format.

1. INTRODUCTION

Climate change and the fast-growing world population are the two main factors that massively affect freshwater accessibility. Infections brought on by dangerous organisms present in water result in 19% of fatalities worldwide, whereas poor water quality causes 80% of illnesses (Wang *et al.* 2022). The threat to the state of the universe as it was evolving was made worse by the difficulty and expense of analysing the chemical and microbial makeup of water. Besides harming human life, polluted water even damages the environment and wildlife (Epelle *et al.* 2022). In the last 20 years, globally, the water pipes connected to residences have augmented, but still, a large group of people have no access to clean drinking water, nearly 780 million (Kamali *et al.* 2019). The water conservation technique is utilized for reducing water usage, but more new solutions are required as conservation is not sufficient because of the needs of the increasing population. Poor sanitation even hinders the supply of safe and clean water (Nizamuddin *et al.* 2019). Hence, new cost-effective and innovative

ways to treat wastewater are vital. The fundamental wastewater treatment process generally includes three main steps: primary, tertiary, and secondary treatment (Kumar 2021).

Negative environmental issues like solid waste management, air pollution, and water pollution are being resolved using nanotechnology (Dutta *et al.* 2022). The more complicated impurities to remove in wastewater lie in a nanoscale range of 1–100 nm; therefore, the nano-based methods are the most suitable techniques. Nanotechnology is very beneficial for water remediation not due to the dimensional field, but then due to its outstanding physicochemical property of nanomaterials (Manimegalai *et al.* 2022). Activated carbon refers to adsorption characterized and its structure of porous, thermostability utilized in numerous applications like the purification of wastewater treatment, removal of impurities, gaseous phases, and odor from medical usage. Using this activated carbon (Guduru *et al.* 2021), adsorption removes the wastewater colours fast and affordably. The treatment of wastewater is complex. Yet, developments in intellectual methods allow them to be used in complex modeling mechanisms (Dang *et al.* 2022). Owing to their robustness, potential applications in engineering and great precision can be used for the improved provision of performance features. Certain indispensable variables can be utilized for assessing the performance of wastewater treatment plants (Xin *et al.* 2021). Such factors are total suspended substances (TSS). TSS are water particles larger than 2 microns. A totally dissolved solid is any particle under 2 mm (TDS). TSS includes algae and bacteria, but most of it is inorganic. TSS includes sand, silt, and plankton. Decomposing plant and animal waste in water sources releases suspended solids. Some silt settles at the bottom of a water source, but other TSS floats or remains suspended. TSS affects water quality. Chemical oxygen demand (COD) is the amount of dissolved oxygen that must be present in water for chemical organic molecules like petroleum to be oxidized. The COD concentration in receiving waters is evaluated to determine the short-term impact of wastewater effluents on the oxygen levels in such waters, and biological oxygen demand (BOD). Biochemical oxygen demand is the dissolved oxygen (DO) aerobic biological organisms need to break down organic material in a water sample at a certain temperature and time. The BOD, calculated as the quantity of oxygen needed per litre of sample after 5 days of incubation at 20 °C, is used to calculate the level of organic contamination in water. Successful wastewater treatment facilities reduce BOD. Wastewater effluent BOD can determine the immediate influence on receiving water oxygen levels. The COD test is less specific because it tests all chemically oxidized organic compounds. Such features were utilized as a model for wastewater treatment plants.

This study develops a new Archimedes optimization algorithm (AOA) with Stacked Sparse Denoising Auto-Encoder (SSDAE) model, named AOA-SSDAE for wastewater management in the IoT environment. The presented AOA-SSDAE technique aims to predict wastewater treatment depending on the influent indicators. In the presented AOA-SSDAE technique, the IoT devices are initially employed for the data collection process and then data normalization is performed for transforming the collected data into a uniform format. Normalization creates clean data. However, data normalization has two purposes: it makes all records and fields look the same. It improves entry type coherence, cleansing, lead creation, segmentation, and data quality. For logical data storage, this procedure eliminates unstructured data and duplicates. Data normalization properly standardizes data entry. The BOD, measured as the amount of oxygen required per litre of the sample after 5 days at 20 °C incubation, is used to quantify the level of organic contamination in water (Gangathimmappa *et al.* 2022). Benefits of data normalization: More storage, more rapidly answered inquiries, improved segmentation, the data must be normalized; there is no other option. For the predictive process, the SSDAE model is applied in this study. For improving the predictive performance of the SSDAE approach, the AOA-based hyperparameter tuning process is involved. A widespread experimental results investigation is conducted to make sure of the improvements of the AOA-SSDAE algorithm.

2. RELATED WORKS

Saka *et al.* (2022) focused on using sunlight for catalyzing the destruction of carbon-based (organic) pollutants. To improve the proficiency of the photocatalytic technique and increase the morphological area, sodium alginate was arranged as a drop practice and utilized as a polymeric tool. SiO_2 nanoparticles have been doped as sodium alginate droplets. The proposed method was capable of spreading the wavelength diversity all over the considerable wavelength constituency. The sunlight catalytic process has been carried out from a photo light droplet or UV–Vis. Soffian *et al.* (2022) investigated a variety of carbon-based materials (CBMs), including biochar, activated carbon, carbon aerogel, graphene, and carbon nanotubes. The generation of dissimilar CBMs and their alteration receives special consideration. As detrimental dyes, organic, and inorganic pollutants evolving from the wastewater have given rise to damage to the water supplies and environment. Adsorption is the more commonly used technique for the deduction of harmful pollutants owing to its usability and comparatively low cost compared to other techniques.

Madhura *et al.* (2019) focused on modern treatment technique with nano-based materials, for instance, carbon and graphene nanotubes, metal nanoparticles including iron, silver, magnesium, and zinc, and magnetic-core composites and metal oxides nanoparticles such as iron, cobalt, and nickel. Moreover, the author compares conventional and emerging techniques for the performance and production cost of organic and inorganic pollutants. Moyo *et al.* (2022) proposed a summary of the dissimilar kinds of nanocellulose utilized in the manufacturing of nanofiber membranes, their properties, and production routes. Ong *et al.* (2018) focused on the recent advancements of carbon-oriented nanocomposite membranes and nanomaterials for the potential treatment of water mixtures or emulsified oil. They also investigated influence of bubble size on the effectiveness of the separation process and the effect that this has on the amount of material removed.

In Dhiman *et al.* (2022), numerous methods for manufacturing carbon-related single-atom catalysts were defined. Following that, an overview of recent advances in a variety of specialized procedures and computer achievements is offered in order to comprehend the geometric and electrical properties of catalysts attached to a single carbon atom. To minimize aquatic pollution, single-carbon atom photocatalysts were used. As single-atom catalysts on carbon particles, many materials are utilized, for example, carbon nitride, graphene, carbon quantum dots, and other materials (Lakshmanna *et al.* 2022). Sawdust, a waste product that is harmful to the environment, was used to construct a novel activated carbon synthesis (Abdel-Salam *et al.* 2020). Magnetite nanoparticles were used to further modify it. Two hydrophilic nanoparticles, silica and bismuth oxide nanomaterials, are included in the nanocomposites Mass Attenuation Coefficient (MAC)/Bi_2O_3 and MAC/SiO_2. Sawdust was microwave-pyrolyzed first, and nanoparticles were added by co-precipitation.

In Xin *et al.* (2021), Fenton-like nanocomposite catalysts made of carbon are employed in microwave, light, electro, and ultrasound Fenton processes. Chemicals are produced and used as a result of industrialization. Organic contaminants in municipal and industrial wastewater are difficult to degrade. They have a huge influence on society if left untreated. More study is needed to better understand Fenton-like processes, how to use them effectively, and how to combine them with artificial intelligence to remediate refractory organic pollutants. Thus, environmental protection necessitates the creation of Fenton-like catalysts. In Manimegalai *et al.* (2023), the agricultural, pharmaceutical, electronic, and environmental industries have all experienced rapid advancements in nanotechnology. The most promising nanotechnology products for electronics and drug delivery are carbon-based nanoparticles because of their distinctive characteristics. Conventional and novel micro/nano-pollutants caused global warming and climate change.

3. THE PROPOSED MODEL

In this study, we have introduced a new AOA-SSDAE technique for wastewater management in the IoT environment. The presented AOA-SSDAE technique aims to predict wastewater treatment depending on the influent indicators. In the presented AOA-SSDAE technique, series of sub-processes are involved, namely data collection, data preprocessing, prediction, and parameter tuning. Figure 1 demonstrates the overall workflow of the AOA-SSDAE approach.

3.1. Data normalization

Firstly, the IoT devices are initially employed for data collection and then data normalization is performed to transform the collected data into a uniform format. Normalization of the inputted values for all attributes computed in the trained instances will support the pace of the up learning stage. The common methods utilized for normalizing processes are *Z*-score normalized, decimal scaling, and Min–Max normalized. Min–Max normalized performed a linear alteration on the actual dataset. $Max\,A$ and $Min\,A$ were the maximal and minimal values of attribute A. Min–Max normalization mapped a value of A to v' in the range by calculating $new\_Min\,A$, $new\_Max\,A$:

$$V' = \frac{V - Min\,A}{Max\,A - Min\,A}(new\_Max\,A - new\_Min\,A) + new\_Min\,A \tag{1}$$

3.2. Prediction using the SSDAE model

In this work, the SSDAE technique was employed for the prediction process. The AE is an unsupervised neural network which reconstructs the vector from the hidden feature space, namely, similar embeddings are kept closer to one another in a hidden space (Asha *et al.* 2022). The procedure of AE can be given in the following: first, a vector was utilized as the input $p^{(k)} \in [0, 1]^m$, which represents the hidden space as $d^{(k)} \in [0, 1]^m$. The encoding functionality parameterized using

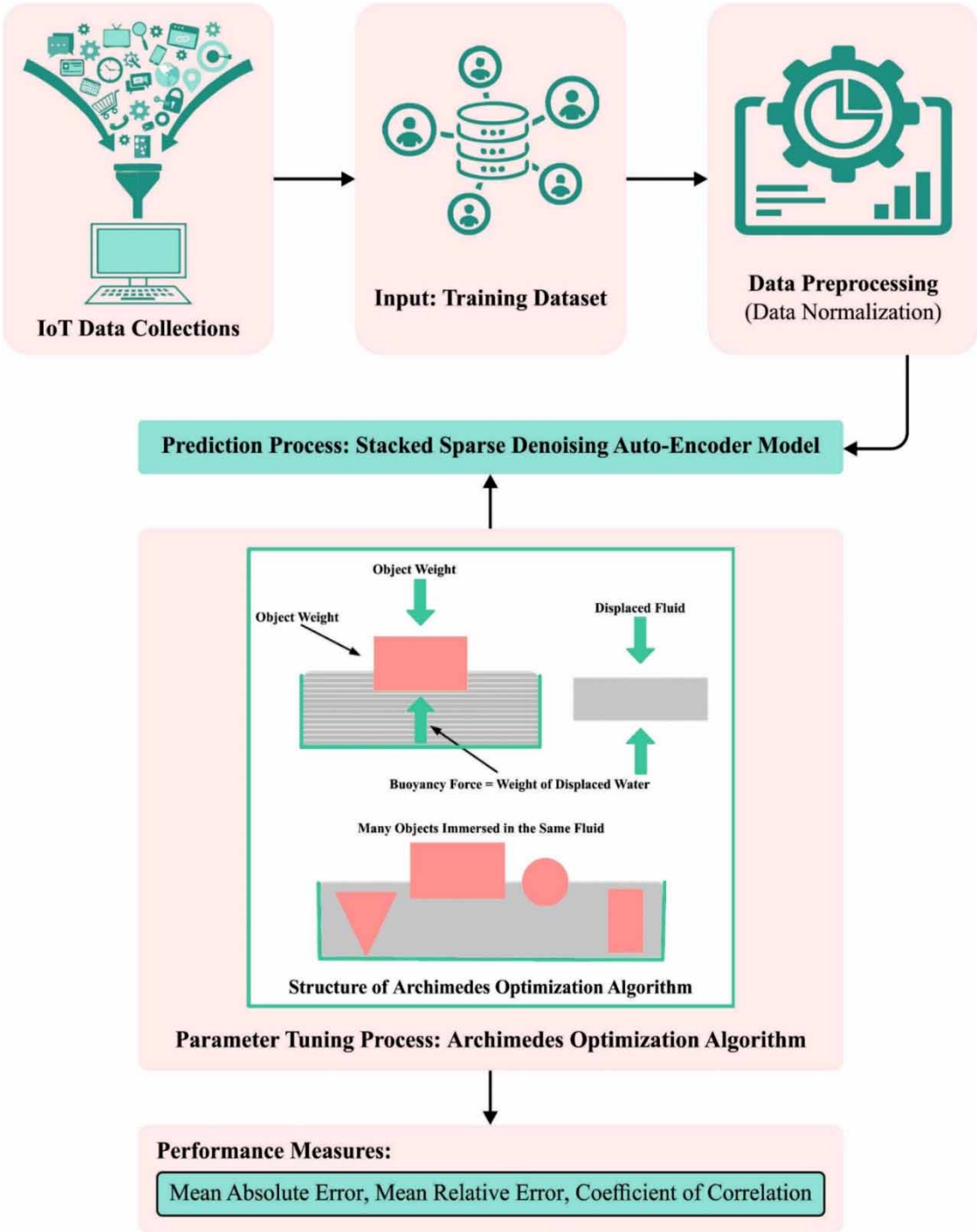

Figure 1 | Overall workflow of the AOA-SSDAE system.

$\theta = \{W,\ b\}$, as follows:

$$d^{(k)} = f\theta(p^{(k)}) = s(Wp^{(k)} + b) \tag{2}$$

where s indicates a non-linear activation function, namely sigmoid function or hyperbolic tangent-, b denotes the bias vector,

and W represents the $m \times m$ weight matrix. The hidden representation $d^{(k)} \in [0, 1]^m$ is later mapped back to the 'reconstructed' vector, $\hat{p} \in [0, 1]^m$, in input space

$$p^{(k)} = g\theta(t^{(k)}) = s(Wt^{(k)} + b) \tag{3}$$

The weight matrix W of the reverse mapping might be optionally constrained using $W = WT$; in such cases, the AE is regarded as having tied weights. The main objective of the training is to learn the parameter $\theta = \{W,\ b\}$, and $\theta' = \{W,\ b\}$ was to decrease the average reconstructed error over a set of input vectors, namely, $p^{(1)}, \ldots, p^{(n)}$

$$(\theta \cdot \theta') = \underset{(\theta \cdot \theta')}{\arg m \max} \frac{1}{n} \sum_{k=1}^{n} Ls(p^{(k)} \cdot p'^{(k)}) \tag{4}$$

$$(\theta \cdot \theta') = \arg m \min_{\theta \cdot \theta'} \frac{1}{n} \sum_{k=0}^{n} Ls(p^{(k)} \cdot g\theta'(f_\theta(p^{(k)}))) \tag{5}$$

Now, Ls indicates the loss function so that cross-entropy θ and θ' parameters are enhanced using mini-batch or stochastic gradient descent. The network will learn the identity function since the autoencoder has been modified to produce a denoising autoencoder (DAE). Or, to put it another way, if the amount of data is too great, the autoencoder may simply learn it and provide results that are similar to the input. The autoencoder in this scenario does not perform any useful representation learning or dimensionality reduction. Autoencoders with denoising capabilities can be used to resolve this problem. To do this, they purposefully change the input data, either by introducing noise or by concealing some of the input values (Neelakandan *et al.* 2022). A DAE is a three-layer neural network which comprises a hidden layer (HL), an input layer, and an output layer. After adding noise to the initial input x, the interference input $\tilde{x}$ is attained, and inputted feature expression h can be attained using the encoding function f_θ. Next, h is mapped to the resultant layer using the decoder function g_θ to achieve the reconstruction data z of the input dataset. The encoder method of DAE is mathematically formulated below:

$$h = f_\theta(\tilde{x}) = \delta(w\tilde{x} + b) \tag{6}$$

where $\theta = (w, b)$ denotes the coding model parameter; w represents the coding weight matrix, and b indicates the coding offset vector. The decoder procedure is mathematically formulated below:

$$z = g_{\theta'}(y) = \delta(w'h + b) \tag{7}$$

where $\theta' = (w', b')$ denotes the decoded model parameter, w' indicates the decoded weight matrix, b' specifies the decoding offset vector, and δ represents the non-linear activation function. The reconstructed outcome z was unable to exactly replicate the input dataset x for the training instance set $D = \{x^{(i)}\}_{i=1}^{N}$, the cost function of DAE is

$$L_{\mathrm{DAE}}(\theta) = \frac{1}{N} \sum_{i=1}^{N} \|z^{(i)} - x^{(i)}\|_F^2 + \frac{\lambda}{2}(\|w\|_F^2 + \|w'\|_F^2) \tag{8}$$

where λ is a weight representation, and lowering the weight lowers overfitting. Additionally, a penalty component was added to the cost function to restrict the level of activation of the neurons responsible for the high-dimension sparse feature

extraction from the input dataset. The sparse DAE (SDAE) cost function can be expressed as a result as

$$L_{\mathrm{SDA}}(\theta) = \frac{1}{N}\sum_{i=1}^{N}\|z^{(i)} - x^{(i)}\|_F^2 + \frac{\lambda}{2}(\|w\|_F^2 + \|w'\|_F^2) + \beta\sum_{j=1}^{k}\left(\rho\log\frac{\rho}{\hat{\rho}_j} + (1-\rho)\log\frac{1-\rho}{1-\hat{\rho}_j}\right)' \tag{9}$$

where ρ reflects the control's sparse restriction weight, whereas β denotes the sparsity parameter and ρ_j denotes the average activation of input dataset equivalent to jth nodes of the HLs. The training of SSDAE adopted the greedy layer-wise training approach that could efficiently mitigate the gradient diffusion phenomenon; i.e., every SDAE is separately trained to attain the optimum weight of the network that is exploited as an SSDAE network weight. Backpropagation is the algorithm for computing the gradient, not how it is employed, although it is sometimes used to refer to the full learning algorithm, including stochastic gradient descent. Backpropagation, a specific case of reverse accumulation, generalizes the gradient calculation in the delta rule, which is the single-layer form of backpropagation. Automatic differentiation generalizes backpropagation. Backpropagation tests for faults from output nodes to input nodes. It improves data mining and machine learning predictions mathematically. Backpropagation calculates derivatives quickly. Then, the network is finetuned by the error backpropagation (BP) technique until the optimum parameter of the networks is derived.

$$L_{\mathrm{SSDAE}}(\theta) = \frac{1}{N}\sum_{i=1}^{N}\|z^{(i)} - x^{(i)}\|_F^2 + \frac{\lambda}{2}\sum_{l=1}^{L}(\|w\|_F^2 + w'\|_F^2) \tag{10}$$

where L identifies the number of SDAE. Although there are no restrictions for sparsity in finetuning, every SDAE's pretraining includes a sparsity penalty. Figure 2 represents the framework of SDAE.

3.3. Hyperparameter tuning process

The Archimedes Optimization Method is a population-based Pigeon Inspired Optimization Algorithm (PIOA) algorithm that is based on the Archimedes principle, a well-known physical fact. Archimedes' principle concisely explains the rule of buoyancy, which determine the relationship between an item immersed in a fluid and the buoyant force exerted on it. If the object's weight is more than the weight of the displaced fluid, it sinks; otherwise, it floats above the fluid in the issue. Finally, the AOA is applied for the optimal hyperparameter tuning of the SSDAE model. AOA can be a population-based metaheuristic physics approach based on Archimedes' rules of buoyancy in water (Geetha *et al.* 2022). AOA exploits the population of an object as a candidate to accomplish a certain objective. AOA initiates by defining how to use the initial population and later starts to reiterate the procedure with certain limits. The search for objects includes the generation of accelerations, volumes, and densities. The AOA was a globally optimal technique that was characterized by mathematical modelling as follows (Raghavendra *et al.* 2022):

Step 1 – Initialization. This includes the initialization of each object's location, volume (*vol*), density (*den*), and acceleration (*acc*) as follows:

$$0_l = lb_l + rand \times (ub_l - lb_l\ l = 1, 2, \ \ldots, \ \mathrm{POP} \tag{11}$$

$$\begin{aligned} den_l &= rand \\ vol_l &= rand \end{aligned} \tag{12}$$

$$acc_l = lb_l + rand \times (ub_l - lb_l) \tag{13}$$

where 0_l signifies the lth objects in the population of Population of N Objects (POP) objects, whereas minimal and maximal limitations of solution space were represented as lb_l and ub_l, correspondingly. *rand* generates random numbers within [0,1] in G-dimension vector. In these steps, the better population is measured, and better fitting objects with maximum fitness values are selected and allocated 0_{best}, den_{best}, vol_{best}, and acc_{best}.

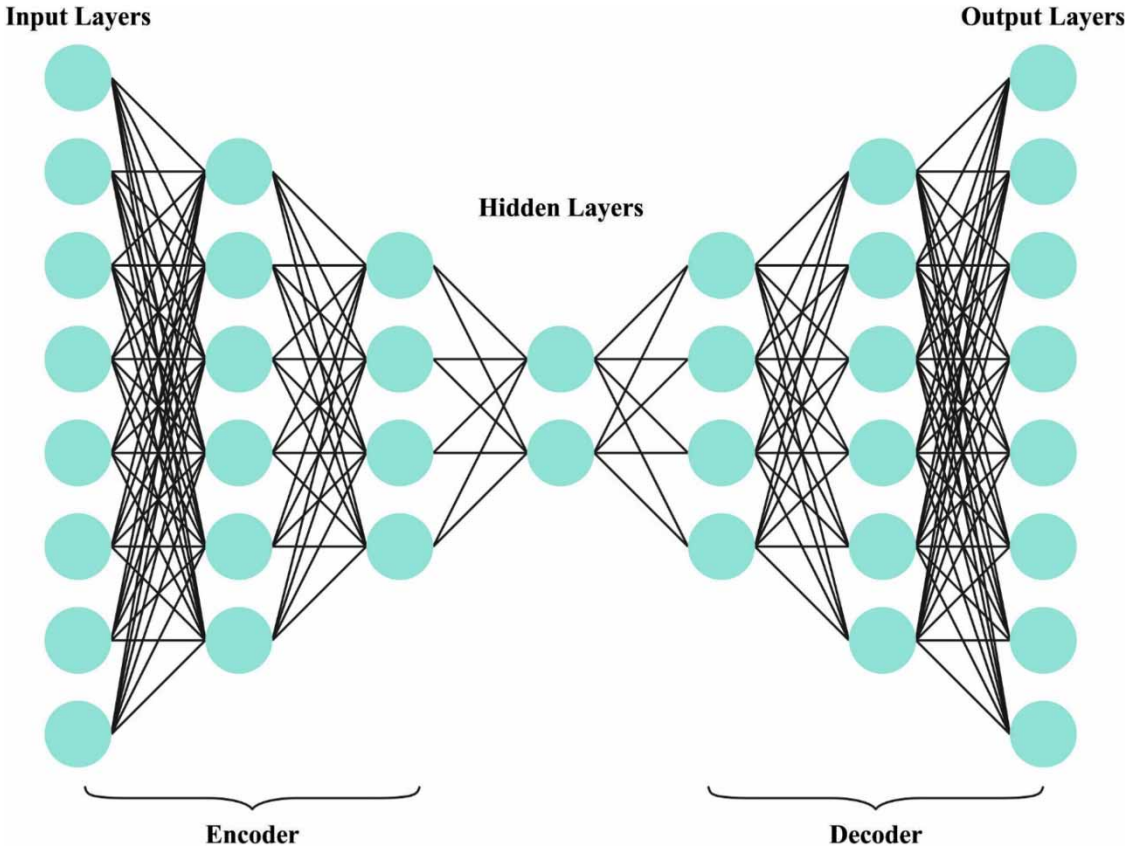

Figure 2 | Architecture of SDAE.

Step 2 – Updates densities and volumes. The volume and density of the items for the following $t+1$ iterations are upgraded and are expressed by:

$$den_l^{t+1} = den_l^t + rand \times (den_{best} - den_l^t) vol_l^{t+1} = vol_l^t + rand \times (vol_{best} - vol_l^t) \tag{14}$$

where *rand* represents the random numeric that is distributed regularly within [0, 1]. den_{best} and vol_{best} denote the volume and density of better objects recognized up to these points.

Step 3 – Transfer operator and density factor (TF). These steps include transfer from exploration to exploiting process. A collision among objects is initiated and, after certain time, the object strives for a state of balance. The TF increases till it attains a constant value and is determined as follows:

$$\mathrm{TP} = \exp\left(\frac{t - t_{\max}}{t_{\max}}\right) \tag{15}$$

where t shows the current iteration count and $t_{\max}$ indicates the maximum number of iterations. TF increases until it reaches 1 over time. The density decreasing factor, (*ddf*), which decreases over time and is determined as follows, is an additional parameter that assists AOA with global-to-local search:

$$ddf^{t+1} = \exp\left(\frac{t_{\max} - t}{t_{\max}}\right) - \left(\frac{t}{t_{\max}}\right) \tag{16}$$

By using iteration, the value of ddf^{t+1} until it reaches a predetermined target location, it lowers with time. AOA allows a better balance between exploration and exploitation if these parameters are well-regulated.

Step 4 – Update the normalization and acceleration of an object. The acceleration of object for the iteration $t+1$ updating procedure acc_l^{t+1} is divided into three stages: 'exploration stage,' 'exploitation stage,' and 'normalized acceleration stage'.

Step 4.1 – Exploration stage (a collision among objects takes place). When TP ≤ 0.5, it specifies a collision between objects, we select the random material (mr) and upgrade the acceleration of the object for $t+1$ iteration as follows:

$$acc_l^{t+1} = \frac{den_{mr} + vol_{mr} \times acc_{mr}}{den_l^{t+1} \times vol_l^{t+1}} \tag{17}$$

where acc_l, $deni_l$, and vol_l represent acceleration, density, and volume, of an object l, correspondingly. acc, den, and vol_{mr}, correspondingly represent density, volume, and acceleration of the random material. Especially, it is necessary to point out that TP ≤ 0.5 allows exploration in one-third of iteration period time. The exploration and exploitation effectiveness is changed once the value except 0.5 is exploited.

Step 4.2 – Exploitation stage (no collision among objects takes place). In the absence of collision (TF > 0.5), the subsequent formula must be used for updating the acceleration of the object at the following iteration, $t+1$:

$$acc_l^{t+1} = \frac{den_{best} + vol_{besi} \times acc_{best}}{den_l^{t+1} \times vol_l^{t+1}} \tag{18}$$

where acc_{besi} signifies the acceleration of an object and is the optimum value.

Step 4.3 – Normalize acceleration. The acceleration can be standardized for computing the alteration percentage as follows:

$$acc_{l-norm}^{t+1} = up \times \frac{acc_l^{t+1} - \min(acc)}{\max(acc) - \min(acc)} + lo \tag{19}$$

where the range of normalization can be determined by $up = 0.9$ and $lo = 0.1$, correspondingly. acc_{l-norm}^{t+1} indicates the proportion of steps that every object changes. The acceleration value is higher if the lth object can be farther from the global optima. On the other hand, it will be in the exploitation stage, namely, representing the progression of search from the exploration stage to the exploitation stage. The AOA was effective to achieve stability regarding exploitation and exploration.

Step 5 – Update location. In the exploration stage (TF ≤ 0.5), the location should be upgraded, where the location of object is adapted for the iteration $t+1$ as follows:

$$b_l^{t+1} = b_l^t + Con_1 \times rand \times acc_{l-norm}^{t+1} \times ddf \times (b_{rand} - b_l^t) \tag{20}$$

where b_l^{t+1} indicates the lth object's upgraded location in a population of POP objects. Con_1 indicates the constant that often equals 2. In the exploitation stage (> 0.5), the object updates the location as:

$$b_l^{t+1} = b_{best}^t + F \times Con_2 \times rand \times acc_{l-norm}^{t+1} \times ddf \times (\mathrm{TR} \times b_{besi} - b_l^t) \tag{21}$$

where Con_2 denotes the constant equivalent to 6. TR progressively increases with time and directly relates to the transfer operator, which is described by TR $= Con_3 \times$ TF. The range of TR is $[Con_3 \times 0.3,\ 1]$, and Con_3 is a constant equivalent to 2. Then, a small proportion is initiated; meanwhile, this causes the step size of random walk to be considerable and the difference between the present and the best locations to be substantial. In the search, this proportion slowly increased to reduce the difference between the actual and the best locations, accomplishing a balance between exploitation and exploration. F shows the item's direction as a flag based on the following expression, which is derived from the object's position:

$$F = \begin{cases} +1, & \text{if } p \leq 0.5 \\ -1, & \text{if } p > 0.5 \end{cases} \tag{22}$$

where $p = 2 \times rand - Con_4$, and Con_4 denotes the constant equivalent to 0.5.

Step 6 – Evaluation. By using iteration, AOA employs the objective function and recognizes the optimum solution for all the objects as the assessment while assigning optimum value to the subsequent parameters: b_{best}, vol_{best}, den_{best}, and acc_{best}. In this study, the AOA was used for determining the hyperparameter indulged in the SSDAE method. The Mean Square Error (MSE) is the objective function and can be defined below:

$$\mathrm{MSE} = \frac{1}{T}\sum_{j=1}^{L}\sum_{i=1}^{M}(y_j^i - d_j^i)^2 \tag{23}$$

where L and M signify the resultant value of data and layer, respectively, d_j^i and y_j^i designate the appropriate and attained magnitudes for jth unit from the resultant layer of network in time t, respectively.

Table 1 | Parameter setting

Parameters	Minimum	Maximum	Average
T-N, mg/dm^3	19.8	99	70.4
T-P, mg/dm^3	3.8	38.6	13.55
BOD, mg/dm^3	40.5	792	378
COD, mg/dm^3	169	2,520	930.1
TSS, mg/dm^3	82	1,145	440
Q, mg/dm^3	26,983	66,883	38,758

Table 2 | Predictive outcome of the AOA-SSDAE approach with existing systems under varying classes

Class	BKNN	ELM	BKNN-ELM	AOA-SSDAE
Mean absolute error (MAE)				
T-N	6.06	7.21	3.98	3.11
T-P	1.62	2.85	1.45	1.04
BOD	45.32	48.15	39.92	35.30
COD	119.21	139.26	109.42	98.87
TSS	57.98	77.93	48.12	45.38
Average	**46.038**	**55.080**	**40.578**	**36.740**
Mean absolute percentage error (MAPE)				
T-N	9.74	12.41	7.56	6.89
T-P	14.07	18.85	11.76	10.76
BOD	14.22	15.04	13.23	12.35
COD	12.98	16.18	10.97	8.37
TSS	16.00	26.21	12.10	11.22
Average	**13.402**	**17.738**	**11.124**	**9.918**
Coefficient of correlation (R)				
T-N	0.76	0.29	0.36	0.28
T-P	0.48	0.54	0.40	0.39
BOD	0.60	0.65	0.61	0.54
COD	0.48	0.40	0.34	0.36
TSS	0.58	0.59	0.43	0.44
Average	**0.580**	**0.494**	**0.428**	**0.402**

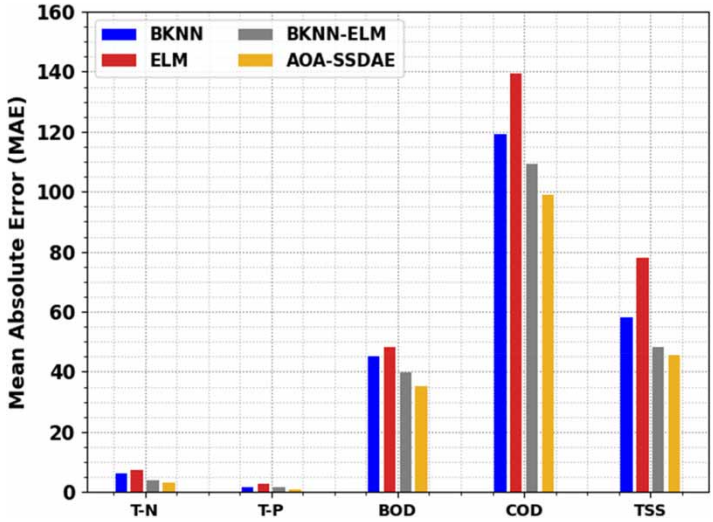

Figure 3 | MAE outcome of the AOA-SSDAE approach under varying classes.

4. RESULTS AND DISCUSSION

In this section, the experimental validation of the AOA-SSDAE technique is tested using the test dataset. Table 1 represents the details of parameter setting.

Table 2 reports an overall predictive outcome of the AOA-SSDAE technique and recent models. Figure 3 investigates a comparative MAE result assessment of the AOA-SSDAE technique with existing models. The results indicated that the AOA-SSDAE technique reaches effectual outcomes with reduced MAE values. For instance, with the T-N class, the AOA-SSDAE technique obtains a lower MAE of 3.11 while the Bobbery set - nearest neighbor (BKNN), Extreme Learning Machine (ELM), and BKNN-ELM models achieve higher MAE of 6.06, 7.21, and 3.98, respectively. Meanwhile, with the BOD class, the AOA-SSDAE technique obtains a lower MAE of 35.30, whereas the BKNN, ELM, and BKNN-ELM techniques accomplish a maximum MAE of 45.32, 48.15, and 39.92, correspondingly. Similarly, with the TSS class, the AOA-SSDAE technique obtains a lower MAE of 45.38, whereas the BKNN, ELM, and BKNN-ELM models accomplish a greater MAE of 57.98, 77.93, and 48.12, correspondingly.

Figure 4 investigates a comparative MAPE result assessment of the AOA-SSDAE technique with current models. The outcomes specified that the AOA-SSDAE technique acquires effectual outcomes with reduced MAPE values. For example, with the T-N

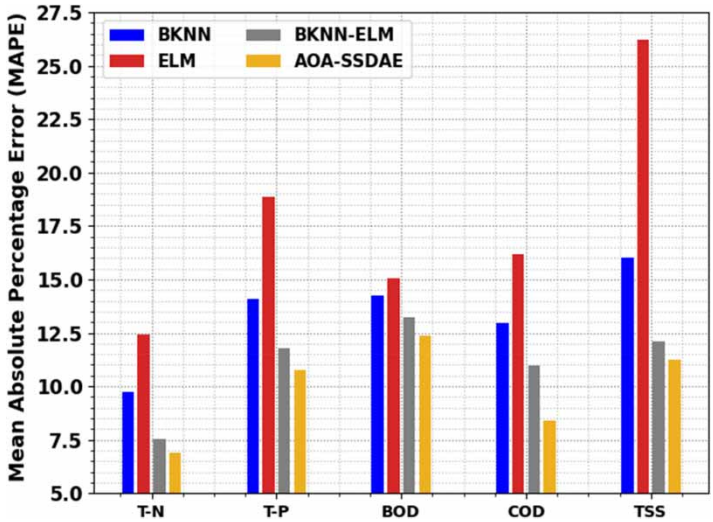

Figure 4 | MAPE outcome of the AOA-SSDAE approach under varying classes.

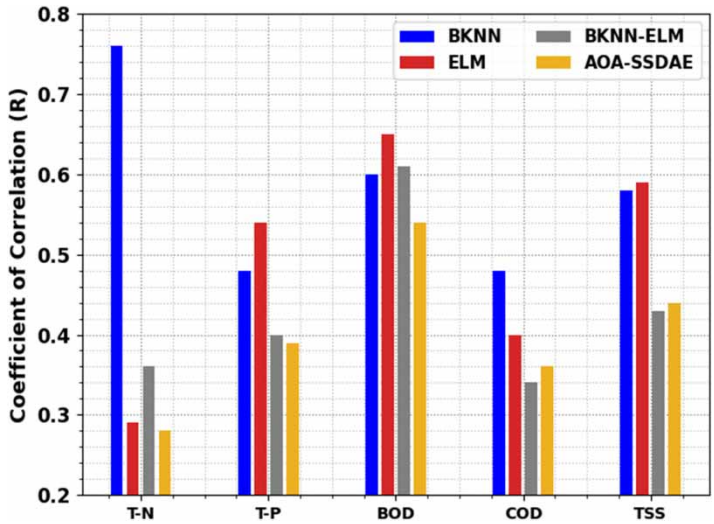

Figure 5 | COC outcome of the AOA-SSDAE approach under varying classes.

class, the AOA-SSDAE technique attains a lower MAPE of 6.89, whereas the BKNN, ELM, and BKNN-ELM models achieve a higher MAPE of 9.74, 12.41, and 7.56, correspondingly. Meanwhile, with the BOD class, the AOA-SSDAE technique reaches a lower MAPE of 12.35, whereas the BKNN, ELM, and BKNN-ELM models attain a higher MAPE of 14.22, 15.04, and 13.23,

Table 3 | Overall outcome of the AOA-SSDAE approach with different measures and runs

No. of runs	$Accu_y$	$Prec_n$	$Reca_l$	F_{Score}
Run-1	97.45	97.27	97.77	97.57
Run-2	97.01	96.78	96.45	96.14
Run-3	96.70	97.20	97.20	97.31
Run-4	96.49	97.27	96.26	96.84
Run-5	96.41	96.19	96.08	96.95
Average	**96.81**	**96.94**	**96.75**	**96.96**

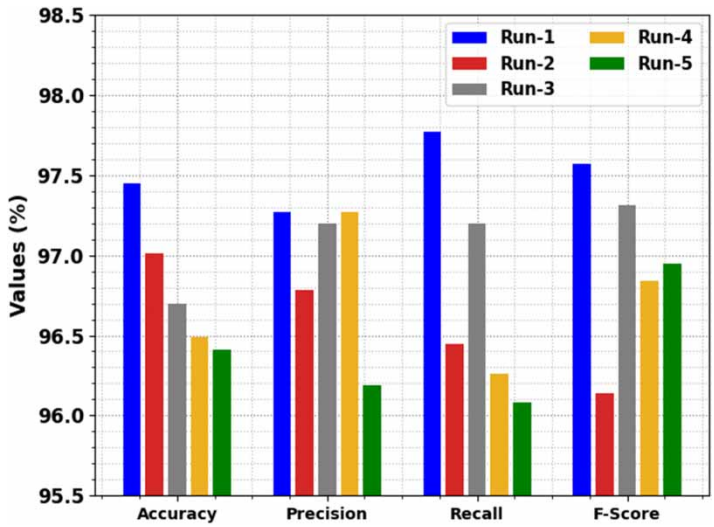

Figure 6 | Overall outcome of the AOA-SSDAE approach with different runs.

correspondingly. Likewise, with the TSS class, the AOA-SSDAE technique acquires a lower MAPE of 11.22 whereas the BKNN, ELM, and BKNN-ELM models accomplish a greater MAPE of 16, 26.21, and 12.10, correspondingly.

Figure 5 examines a comparative Coefficient of Correlation (COC) result assessment of the AOA-SSDAE technique with existing models. The results showed that the AOA-SSDAE technique accomplishes effectual outcomes with reduced COC values. For example, with the T-N class, the AOA-SSDAE method gains a minimum COC of 0.28, whereas the BKNN, ELM, and BKNN-ELM models achieve a maximum COC of 0.76, 0.29, and 0.36, correspondingly. Meanwhile, with the BOD class, the AOA-SSDAE method achieves a lower COC of 0.54, whereas the BKNN, ELM, and BKNN-ELM models achieve a higher COC of 0.60, 0.65, and 0.61, correspondingly. Likewise, with the TSS class, the AOA-SSDAE technique reaches a lower COC of 0.44, whereas the BKNN, ELM, and BKNN-ELM models achieve a greater COC of 0.58, 0.59, and 0.43, correspondingly.

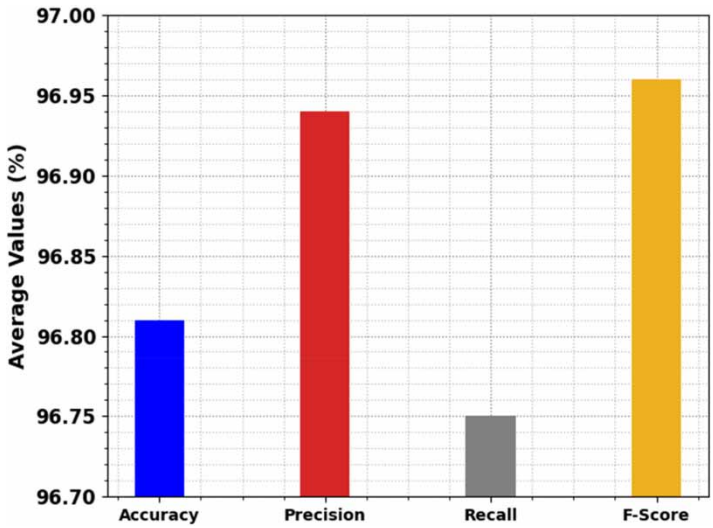

Figure 7 | Average outcome of the AOA-SSDAE approach with different runs.

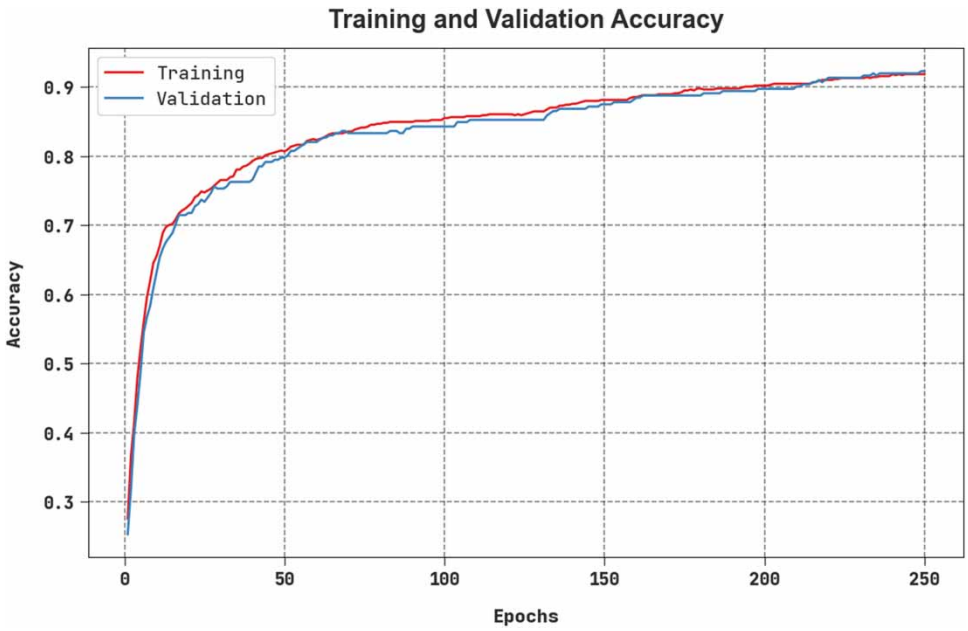

Figure 8 | TACY and VACY outcome of the AOA-SSDAE system.

In Table 3 and Figure 6, an overall result analysis of the AOA-SSDAE technique is examined under five distinct runs. The results inferred that the AOA-SSDAE technique obtained effectual outcomes under each run. For the sample, with run-1, the AOA-SSDAE system reaches $accu_y$ of 97.45%, $prec_n$ of 97.27%, $reca_l$ of 97.77%, and F_{score} of 97.57%. Simultaneously, with run-3, the AOA-SSDAE technique reaches $accu_y$ of 96.70%, $prec_n$ of 97.20%, $reca_l$ of 97.20%, and F_{score} of 97.31%. Concurrently, with run-4, the AOA-SSDAE technique achieves $accu_y$ of 96.49%, $prec_n$ of 97.27%, $reca_l$ of 96.26%, and F_{score} of 96.84%. Finally, with run-5, the AOA-SSDAE technique obtains $accu_y$ of 96.41%, $prec_n$ of 96.19%, $reca_l$ of 96.08%, and F_{score} of 96.95%.

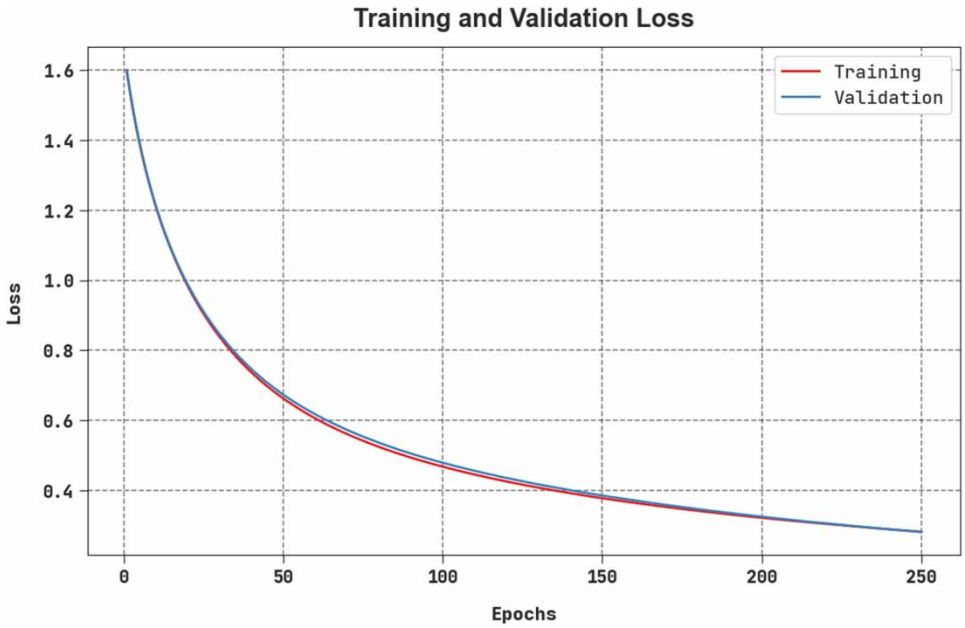

Figure 9 | TLOS and VLOS outcome of the AOA-SSDAE system.

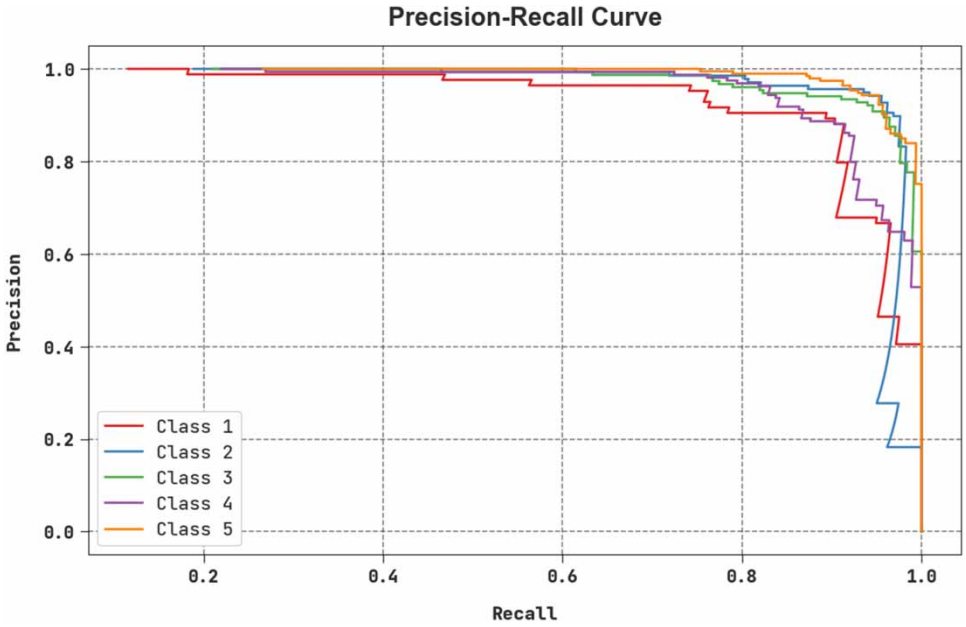

Figure 10 | Precision-recall outcome of the AOA-SSDAE approach.

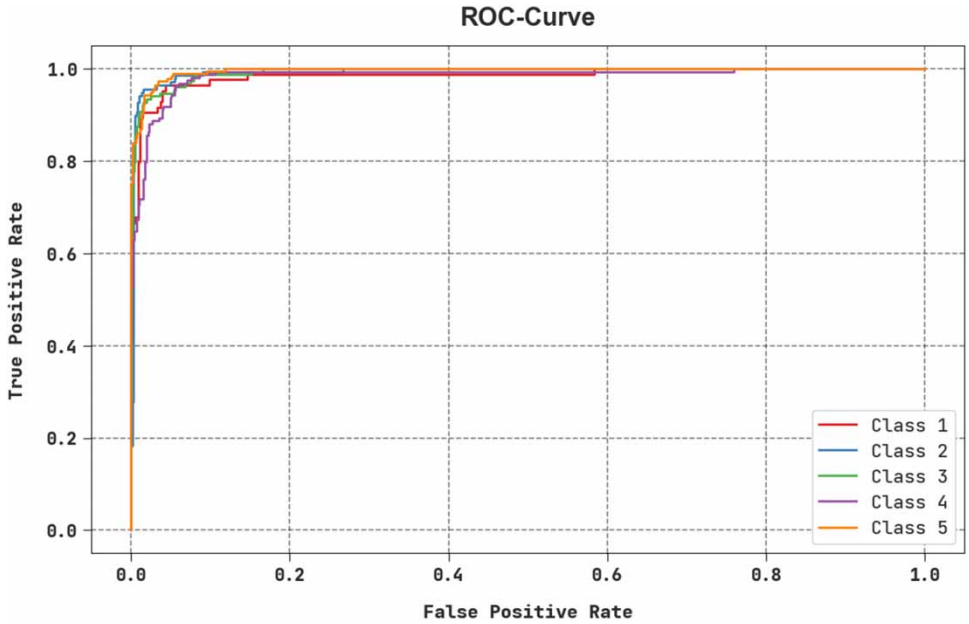

Figure 11 | ROC outcome of the AOA-SSDAE approach.

A brief average result investigation of the AOA-SSDAE technique is portrayed in Figure 7. The results indicated that the AOA-SSDAE technique showed effectual outcomes under each run. It is observed that the AOA-SSDAE technique accomplishes average $accu_y$ of 96.81%, $prec_n$ of 96.94%, $reca_l$ of 96.75%, and F_{score} of 96.96%.

The Training Accuracy (TACY) and Validation Accuracy (VACY) of the AOA-SSDAE technique are examined in wastewater treatment performance in Figure 8. The figure inferred that the AOA-SSDAE method has shown enhanced performance with enhanced values of TACY and VACY. It is noted that the AOA-SSDAE approach has gained maximal TACY outcomes.

The Training Loss (TLOS) and Validation Loss (VLOS) of the AOA-SSDAE method are tested on wastewater treatment performance in Figure 9. The figure demonstrated that the AOA-SSDAE approach has revealed improved performance with minimum values of TLOS and VLOS. It is noted that the AOA-SSDAE system has resulted in lower VLOS outcomes.

An evident precision-recall inspection of the AOA-SSDAE technique under test database is depicted in Figure 10. The figure specified that the AOA-SSDAE system has led to enhanced values of precision-recall values in five classes.

A detailed Receiver Operating Characteristic (ROC) study of the AOA-SSDAE technique under test database is described in Figure 11. The outcomes symbolized the AOA-SSDAE methodology has demonstrated its capability to classify distinct five classes.

Finally, Table 4 and Figure 12 represent an overall comparison study of the AOA-SSDAE technique with other existing models (Faritha Banu *et al.* 2022). The experimental values notified that the ELM model reaches least outcomes with $accu_y$ of 79.19%, $prec_n$ of 90.17%, and $reca_l$ of 90.14%. In addition, the BKNN model obtains slightly improvised outcomes with $accu_y$ of 88.14%, $prec_n$ of 78.16%, and $reca_l$ of 72.19%. Moreover, the BKNN-ELM model obtains reasonable performance with $accu_y$ of 96.20%, $prec_n$ of 94.12%, and $reca_l$ of 93.19%. However, the AOA-SSDAE

Table 4 | Comparative analysis of the AOA-SSDAE system with other methods

Methods	Accuracy	Precision	Recall
BKNN	88.14	78.16	72.19
ELM	79.19	90.17	90.14
BKNN-ELM	96.20	94.12	93.19
AOA-SSDAE	96.81	96.94	96.75

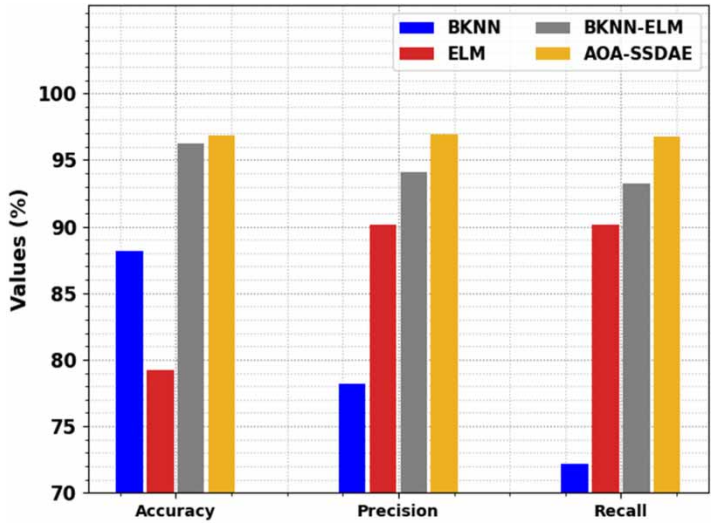

Figure 12 | Comparative analysis of the AOA-SSDAE system with other methods.

technique accomplishes better performance with $accu_y$ of 96.81%, $prec_n$ of 96.94%, and $reca_l$ of 96.75%. These results ensured that the AOA-SSDAE technique accomplished the maximum performance with $accu_y$ of 96.81%, $prec_n$ of 96.94%, and $reca_l$ of 96.75%.

5. CONCLUSION

In this study, we introduce a novel AOA-SSDAE technique for wastewater management in an IoT setting. The presented AOA-SSDAE technique aims to predict wastewater treatment depending on the influent indicators. In the presented AOA-SSDAE technique, a series of sub-processes are involved, namely data collection, data preprocessing, prediction, and parameter tuning. Primarily, the IoT devices are initially employed for data collection process and then data normalization is performed for transforming the collected data into a uniform format. For the predictive process, the SSDAE model is applied in this research. For the SSDAE model's prediction capability to be improved, the AOA-based hyperparameter tuning process is involved. A widespread experimental results analysis is made to ensure the improvements of the AOA-SSDAE system. The AOA-SSDAE methodology, which has a 96.81% accuracy rate, can provide better results. A detailed comparison study revealed that the AOA-SSDAE technique outperformed other modern models. To ensure that the AOA-SSDAE system will be able to be improved even further in the future, further enhancements will make use of more advanced methods.

ACKNOWLEDGEMENTS

A.A.G. is grateful to the Researchers Supporting Project number (RSP2023R407), King Saud University, Riyadh, Saudi Arabia, for the support.

DATA AVAILABILITY STATEMENT

All relevant data are included in the paper or its Supplementary Information.

CONFLICT OF INTEREST

The authors declare there is no conflict.

REFERENCES

Abdel-Salam, M. O., Younis, S. A., Moustafa, Y. M., Al-Sabagh, A. M. & Khalil, M. M. 2020 Microwave-assisted production of hydrophilic carbon-based magnetic nanocomposites from saw-dust for elevating oil from oil field wastewater. *Journal of Cleaner Production* **249**, 119355.

Asha, P., Natrayan, L., Geetha, B. T., Rene Beulah, J., Sumathy, R., Varalakshmi, G. & Neelakandan, S. 2022 IoT enabled environmental toxicology for air pollution monitoring using AI techniques. *Environmental Research* **205**, 112574. https://doi.org/10.1016/j.envres.2021.112574.

Dang, Y. T., Gangadoo, S., Truong, V. K., Cozzolino, D. & Chapman, J. 2022 New nanomaterials for wastewater depollution: methods using chemometric approaches. *Separation Science and Technology* **15**, 287–298.

Dhiman, P., Goyal, D., Rana, G., Kumar, A., Sharma, G. & Kumar, G. 2022 Recent advances on carbon-based nanomaterials supported single-atom photo-catalysts for wastewater remediation. *Journal of Nanostructure in Chemistry*, 1–32.

Dutta, V., Verma, R., Gopalkrishnan, C., Yuan, M. H., Batoo, K. M., Jayavel, R., Chauhan, A., Lin, K. Y. A., Balasubramani, R. & Ghotekar, S. 2022 Bio-inspired synthesis of carbon-based nanomaterials and their potential environmental applications: a state-of-the-art review. *Inorganics* **10** (10), 169.

Epelle, E. I., Okoye, P. U., Roddy, S., Gunes, B. & Okolie, J. A. 2022 Advances in the applications of nanomaterials for wastewater treatment. *Environments* **9** (11), 141.

Faritha Banu, J., Neelakandan, S., Geetha, B. T., Selvalakshmi, V., Umadevi, A. & Martinson, E. O. 2022 Artificial intelligence based customer churn prediction model for business markets. *Computational Intelligence and Neuroscience* **2022**. https://doi.org/10.1155/2022/1703696.

Gangathimmappa, M., Subramani, N., Sambath, V., Ramanujam, R. A. M. & Sammeta, M. 2022 Deep learning enabled cross-lingual search with metaheuristic web-based query optimization model for multi-document summarization. *Concurrency Computation Practice Experience*, e7476. doi:10.1002/cpe.7476.

Geetha, B. T., Kumar, P. S., Bama, B. S., Neelakandan, S., Dutta, C. & Babu, D. V. 2022 Green energy aware and cluster-based communication for future load prediction in IoT. *Sustainable Energy Technologies and Assessments* **52**, 102244. https://doi.org/10.1016/j.seta.2022.102244.

Guduru, R. K., Gupta, A. A., Pillai, P. & Dharaskar, S. 2021 Applications of carbon-based nanomaterials for wastewater treatment. *Environmental Applications of Carbon Nanomaterials-Based Devices*, 87–133.

Kamali, M., Persson, K. M., Costa, M. E. & Capela, I. 2019 Sustainability criteria for assessing nanotechnology applicability in industrial wastewater treatment: current status and future outlook. *Environment International* **125**, 261–276.

Kumar, S. 2021 Carbon based nanomaterial for removal of heavy metals from wastewater: a review. *International Journal of Environmental Analytical Chemistry* **312**, 1–18.

Lakshmanna, K., Subramani, N., Alotaibi, Y., Alghamdi, S., Khalafand, O. I. & Nanda, A. K. 2022 Improved metaheuristic-driven energy-aware cluster-based routing scheme for IoT-assisted wireless sensor networks. *Sustainability* **14**, 7712. https://doi.org/10.3390/su14137712.

Madhura, L., Singh, S., Kanchi, S., Sabela, M. & Bisetty, K. 2019 Nanotechnology-based water quality management for wastewater treatment. *Environmental Chemistry Letters* **17** (1), 65–121.

Manimegalai, S., Vickram, S., Deena, S. R., Rohini, K., Thanigaivel, S., Manikandan, S., Subbaiya, R., Karmegam, N., Kim, W. & Govarthanan, M. 2023 Carbon-based nanomaterial intervention and efficient removal of various contaminants from effluents – a review. *Chemosphere* **312** (Part 1), 137319. https://doi.org/10.1016/j.chemosphere.2022.137319.

Moyo, S., Gumbi, N. N., De Kock, L. A. & Nxumalo, E. N. 2022 A mini-review of nanocellulose-based nanofiber membranes incorporating carbon nanomaterials for dye wastewater treatment. *Environmental Nanotechnology, Monitoring & Management* **18**, 100714.

Neelakandan, S., Prakash, M., Geetha, B. T., Nanda, A. K., Metwally, A. M., Santhamoorthy, M. & Gupta, M. S. 2022 Metaheuristics with Deep Transfer Learning Enabled Detection and classification model for industrial waste management. *Chemosphere*, 136046. https://doi.org/10.1016/j.chemosphere.2022.136046.

Nizamuddin, S., Siddiqui, M. T. H., Mubarak, N. M., Baloch, H. A., Abdullah, E. C., Mazari, S. A., Griffin, G. J., Srinivasan, M. P. & Tanksale, A. 2019 Iron oxide nanomaterials for the removal of heavy metals and dyes from wastewater. *Nanoscale Materials in Water purification* **17**, 447–472.

Ong, C. S., Al-Anzi, B. S. & Lau, W. J. 2018 Recent developments of carbon nanomaterials-incorporated membranes, carbon nanofibers and carbon membranes for oily wastewater treatment. In: *Carbon-based Polymer Nanocomposites for Environmental and Energy Applications* (A. Fauzi Ismail, P. S. Goh, eds.). Universiti Teknologi Malaysia (UTM), Johor Bahru, Malaysia, pp. 261–280.

Raghavendra, S., Neelakandan, S., Prakash, M., Geetha, B. T., Asha, S. M. & Roberts, M. K. 2022 Artificial humming bird with data science enabled stability prediction model for smart grids. *Sustainable Computing: Informatics and Systems* **36**. https://doi.org/10.1016/j.suscom.2022.100821.

Saka, A., Tesfaye, J. L., Gudata, L., Karthi, S., Nagaprasad, N., Bhagat, S. K., Yaqub, M. & Ramaswamy, K. 2022 Polymeric droplets on SiO_2 nanoparticles through wastewater treatment of carbon-based contaminants in photocatalytic degradation. *Journal of Nanomaterials* **2022**, 1–11.

Soffian, M. S., Halim, F. Z. A., Aziz, F., Rahman, M. A., Amin, M. A. M. & Chee, D. N. A. 2022 Carbon-based material derived from biomass waste for wastewater treatment. *Environmental Advances* **9**, 100259.

Wang, G., Su, W., Hu, B., Al-Huqail, A. A., Majdi, H. S., Algethami, J. S., Jiang, Y. & Ali, H. E. 2022 Assessment in carbon-based layered double hydroxides for water and wastewater: application of artificial intelligence and recent progress. *Chemosphere* **308**, 136303.

Xin, L., Hu, J., Xiang, Y., Li, C., Fu, L., Li, Q. & Wei, X. 2021 Carbon-based nanocomposites as Fenton-like catalysts in wastewater treatment applications: a review. *Materials* **14** (10), 2643. https://doi.org/10.3390/ma14102643.

First received 16 January 2023; accepted in revised form 9 April 2023. Available online 4 May 2023